

Manganese dioxide–carbon nanotube nanocomposites for electrodes of electrochemical supercapacitors

Yaohui Wang,^a Hao Liu,^b Xueliang Sun^b and Igor Zhitomirsky^{a,*}

^aDepartment of Materials Science and Engineering, McMaster University, 1280 Main Street West, Hamilton, Ont., Canada L8S 4L7

^bDepartment of Mechanical and Materials Engineering, University of Western Ontario, London, Ont., Canada N6A 5B9

Received 21 July 2009; revised 23 August 2009; accepted 28 August 2009

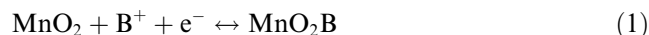
Available online 1 September 2009

Electrodes for electrochemical supercapacitors were fabricated by cathodic electrodeposition of MnO₂ on carbon nanotubes (CNTs), which were grown by chemical vapour deposition on stainless steel meshes. The MnO₂–CNT nanocomposites were characterized by scanning electron microscopy, transmission electron microscopy, cyclic voltammetry and impedance spectroscopy. The electrodes showed excellent capacitive behaviour in the 0.5 M Na₂SO₄ electrolyte, with specific capacitance of 356 F g⁻¹ at a scan rate of 2 mV s⁻¹.

© 2009 Acta Materialia Inc. Published by Elsevier Ltd. All rights reserved.

Keywords: Manganese dioxide; Carbon nanotubes; Nanocomposites; Electrochemical supercapacitor

MnO₂ has been considered as a promising electrode material for electrochemical supercapacitors (ESs) because of its low cost and excellent capacitive performance in the aqueous electrolytes [1–3]. The charging mechanism of MnO₂ is described by the following reaction [4,5]:

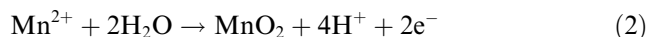


where B⁺ = Li⁺, Na⁺, K⁺, H⁺. Eq. (1) indicates that the large surface area and high ionic and electronic conductivity of the electrode material are necessary in order to utilize the high theoretical specific capacitance (SC) (1380 F g⁻¹) of MnO₂ [3]. Impressive progress has been achieved in the fabrication of fine MnO₂ powders with a large surface area [6–8]. Different types of manganese dioxides have been investigated, including amorphous and nanocrystalline phases [1,9,10]. Thin MnO₂ films [11,12] exhibited an SC of ~700 F g⁻¹. However, the SC decreased with increasing film thickness due to the low conductivity of MnO₂. The values of SC reported in the literature [13,14] are usually in the range between 100 and 250 F g⁻¹.

Recent studies highlighted the influence of the electrode porosity on the electrochemical performance [15–17]. The porous structure of MnO₂ is beneficial for the ion (B⁺) access to the surface of this material. Fur-

thermore, many successful efforts have been made in the area of the fabrication of composite materials, where improved electronic conductivity has been achieved by the use of CNTs and other conductive additives [18–21].

Significant interest has been generated in application of electrochemical methods for the fabrication of MnO₂–CNT composite electrodes. CNTs were deposited on platinized silicon wafers and then impregnated with MnO₂ using anodic electrodeposition [22]. The anodic electrodeposition method was based on the use of Mn²⁺ species, which were oxidized in the anodic reaction:



In another study [23], Mn hydroxide was deposited cathodically from the Mn²⁺ solutions on the CNTs formed on the graphite substrate and converted to MnO₂ after annealing in air at 350 °C. It should be noted that anodic electrodeposition from the solutions of Mn²⁺ salts offers the advantage of room-temperature processing. However, anodic electrodeposition of MnO₂ on stainless steel and other low-cost metallic substrates presents difficulties, related to the anodic oxidation and dissolution of the substrates. As a result of the anodic dissolution of the substrates, the precise measurement of the mass of the deposited MnO₂ and the calculation of SC present difficulties [24]. This problem was addressed by the use of Ta substrates [24], which were stable in the MnSO₄ solutions during anodic electrodeposition. CNT arrays [24] were grown on the Ta substrates by the

* Corresponding author. Tel.: +1 905 525 9140; fax: +1 905 528 9295; e-mail: zhitom@mcmaster.ca

chemical vapour deposition (CVD) method. The CNTs grown directly on the Ta current collectors of ESs offered the advantage of low contact resistance, which was important for the fabrication of efficient ESs with high charge–discharge rates. Another advantage of this approach was binder-free processing, since the use of binder for the fabrication of composite electrodes results in increased resistance and reduced SC [24].

The problem related to anodic oxidation and dissolution of metallic current collectors can be avoided using the cathodic electrodeposition method, which we developed in our previous investigations [16,17,25]. In this method, MnO₂ films were obtained by cathodic reduction of Mn⁷⁺ species from KMnO₄ or NaMnO₄ solutions, using the following reaction:



The films were obtained on stainless steel substrates and exhibited capacitive behavior in the Na₂SO₄ electrolyte. The goal of this investigation was the fabrication of composite MnO₂–CNT electrodes using the cathodic electrodeposition method. CNTs were grown by the CVD method on the stainless steel mesh substrates and impregnated with MnO₂ by cathodic electrodeposition from KMnO₄ solutions.

The microstructure of CNTs formed on the current collectors is important for the fabrication of MnO₂–CNT electrodes. According to Zhang et al. [24], the electrodeposition of MnO₂ on the dense arrays of parallel CNTs, formed on the flat Ta foil substrates, presented difficulties due to the limited ion access to the CNT surface and electrical shielding effect of the dense arrays of conductive CNTs. Zhang et al. reported that MnO₂ particles with a nanoflower microstructure formed only at the junctions of the individual CNTs.

In previous investigations [26,27] it was shown that relatively low density CNT arrays can be formed by CVD. As an extension of the previous investigations, the CVD method was utilized for the CNTs growth on stainless steel meshes and the formation of porous CNT microstructures. The formation of CNTs on thin wires of the stainless steel meshes offered additional benefits. In this case, the growth of parallel CNT arrays can be avoided. Moreover, the high surface area of the current collectors, containing CNTs grown on meshes, was beneficial for the ion access during electrodeposition of MnO₂ from the KMnO₄ solutions and testing of the MnO₂ deposited on the current collectors in the Na₂SO₄ solutions.

The microstructures of the CNTs and MnO₂–CNT nanocomposites were investigated using a JEOL JSM-

7000F scanning electron microscope and a Philips CM10 transmission electron microscope. Capacitive behaviour of the MnO₂–CNT nanocomposites was studied using a potentiostat (PARSTAT 2273, Princeton Applied Research) controlled by a computer using a PowerSuite electrochemical software. Electrochemical studies were performed using a standard three-electrode cell containing 0.5 M Na₂SO₄ aqueous solution, degassed with purified nitrogen gas. The surface area of the working electrodes was 1 cm². The counter electrode was a platinum gauze, and the reference electrode was a standard calomel electrode (SCE). Cyclic voltammetry (CV) studies were performed within a potential range of 0–0.9 V vs. SCE at scan rates of 2–100 mV s⁻¹. The SC was calculated using half the integrated area of the CV curve to obtain the charge, and subsequently dividing the charge by the mass of MnO₂ and the width of potential window. Impedance spectroscopy investigations were performed in the frequency range of 0.1 Hz–100 kHz at a voltage of 5 mV. Simulations of the impedance behaviour were performed on the basis of the equivalent-circuit models using ZsimpWin 3.10 commercial software.

Figure 1 shows typical scanning electron microscopy (SEM) images of CNTs grown on the stainless steel mesh substrates. The SEM images at different magnifications (Fig. 1a and b) indicated that CNTs were randomly oriented and formed a porous network. The CNTs totally cover the wires of the meshes and have a length of about 10 μm. Transmission electron microscopy (TEM) studies (Fig. 1c) showed that the diameter of multiwalled CNTs is about 70–80 nm.

The use of meshes as substrates and porous microstructure of the randomly oriented CNTs offered the advantage of improved access of MnO₄⁻ ions to the CNT surface compared to the dense arrays of vertically aligned parallel CNTs [24] formed on the foil substrates. The cathodic electrodeposition was performed from aqueous 20 mM KMnO₄ solutions using 10 × 10 mm substrates at a constant current of 8 mA. The deposition mechanism, kinetics of deposition, structure and composition of the MnO₂ formed by cathodic electrosynthesis were described in the previous investigations [16,17,25]. Figure 2 shows the SEM images of the electrodes after cathodic electrodeposition. Similar to the literature data on anodic electrodeposition, we observed enhanced deposition at the CNT junctions (Fig. 2a). However, SEM images indicated that MnO₂ particles were also deposited on individual CNTs and CNT bundles (Fig. 2b). The SEM image at higher magnification showed that particle size of MnO₂ was in the range of

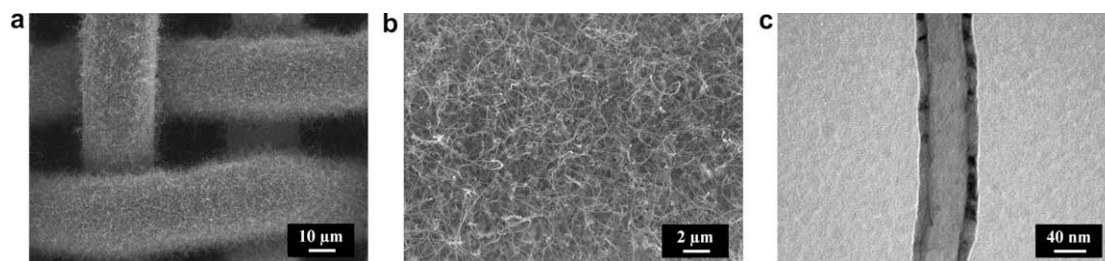


Figure 1. (a and b) SEM images at different magnifications of CNTs on stainless steel mesh and (c) TEM image of individual CNT.

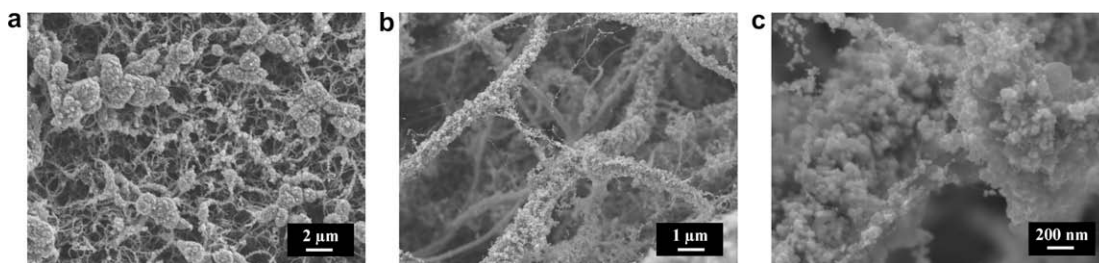


Figure 2. (a–c) SEM images at different magnifications of MnO₂-CNT nanocomposites.

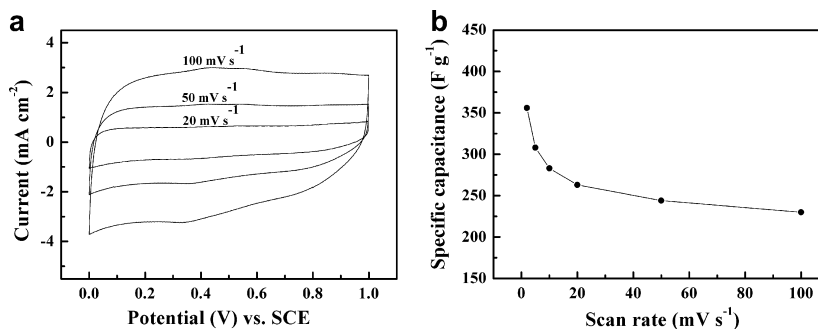


Figure 3. (a) CVs at scan rates of 20, 50 and 100 mV s⁻¹ for the MnO₂-CNT nanocomposites on stainless steel mesh and (b) SC vs. scan rate for the MnO₂-CNT nanocomposites. The variability in data between samples prepared under similar conditions was in the range of $\pm 5\%$.

30–50 nm. This is in a good agreement with the results of the previous investigations [16,17], which showed the formation of nanostructured MnO₂ by the cathodic electrodeposition method.

Figure 3a shows CVs for MnO₂-CNT nanocomposites at different scan rates. The box-shape CVs at different scan rates showed good capacitive behaviour. It is suggested that the porous structure of the MnO₂-CNT electrodes (Fig. 2) was beneficial for the electrolyte access to the active material, whereas CNTs provided improved electronic conductivity. Turning again to Eq. (1), it should be noted that the improved electrolyte access to the active material and good electronic conductivity of the CNT support enabled relatively high SC. The SCs calculated from CVs at different scan rates are shown in Figure 3b. The MnO₂-CNT nanocomposites with a film mass of 120 $\mu\text{m}^2\text{cm}^{-2}$ exhibited an SC of 356 F g⁻¹ at a scan rate of 2 mV s⁻¹ and an SC of 230 F g⁻¹ at a scan rate of 100 mV s⁻¹.

In a previous investigation [16] it was found that the 45 $\mu\text{g cm}^{-2}$ film prepared by cathodic electrodeposition

on stainless steel foil substrates exhibited an SC of 353 F g⁻¹ at a scan rate of 2 mV s⁻¹. However, at a scan rate of 100 mV s⁻¹ the SC was only 135 F g⁻¹. The increase in the film's mass resulted in a significant reduction in the SC. The SC of a 100 $\mu\text{g cm}^{-2}$ film on a stainless steel foil was 263 and 86 F g⁻¹ for scan rates of 2 and 100 F g⁻¹, respectively [16]. The results of our investigation indicate that the use of CNT-modified stainless steel mesh substrates allowed a higher SC, especially at high scan rates. The improved capacitive behaviour of the MnO₂-CNT nanocomposites can be attributed to their lower electrical resistance.

Figure 4a shows complex impedance data of the MnO₂-CNT nanocomposites. The equivalent circuit of the ES included an RC transmission line, describing the porous electrode [28]. C_n elements represented double layer capacitance and pseudo capacitance, whereas R_n elements represented electrolyte resistance in pores, Faradaic resistance and equivalent series resistance of the electrodes. Conway and Pell [29] described the impedance of porous electrode using a five-element

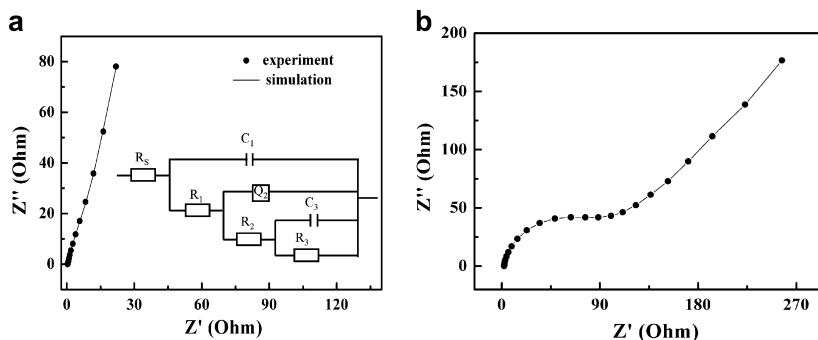


Figure 4. Nyquist plots of the complex impedance $Z^* = Z' - iZ''$ for (a) the MnO₂-CNT nanocomposite and (b) MnO₂ with MnO₂ film mass of 120 $\mu\text{m}^2\text{cm}^{-2}$ on a stainless steel mesh. The variability in data between samples prepared under similar conditions was in the range of $\pm 5\%$.

($n = 5$) circuit. A constant phase element Q , describing a “leaking” capacitor with microscopic roughness of the surface and capacitance dispersion of interfacial origin, was used in this investigation instead of a pure capacitance C . Solutions resistance R_S is usually combined in series with the RC transmission line. The equivalent circuits should allow an optimum representation of the measured spectra with a minimum set of model parameters. Good agreement of simulated and measured voltage data (Fig. 4a) was found for the equivalent circuit containing a transmission line with three RC (Q) elements. The high frequency value of the real part of complex impedance has been used for the estimation of equivalent series resistance, which was found to be $\sim 0.4 \Omega$.

In order to investigate the influence of CNT on the resistance of the electrode material, manganese dioxide films were deposited on stainless steel mesh. Figure 4a and b compares the impedance data in the frequency range of 0.1 Hz–100 kHz for the manganese dioxide films of the same mass deposited on mesh substrates with and without CNT. The results indicated that the samples containing CNT showed significantly lower resistance compared to the sample without CNT. Moreover, the manganese dioxide–CNT composites prepared by the combined electrodeposition–CVD method on the mesh substrates showed lower resistance and higher capacitance compared to the manganese dioxide–CNT films prepared by electrophoretic deposition on stainless steel foils [30]. It is important to note that the electrodeposition method used in this investigation included electrosynthesis of nanoparticles in situ in electrode reaction from the KMnO_4 solutions and film deposition. In contrast, the electrophoretic method [30] was based on the use of suspensions of manganese dioxide nanoparticles. The nanoparticles were charged and dispersed in the solvent using alginic acid as a charging agent [30]. Electrochemical deposition offers the advantage of smaller particle size and agglomerate-free processing of nanomaterials [31]. Another advantage of the method developed in this investigation compared to Ref. [30] is related to the cathodic processing of manganese dioxide. The SC of 200 F g^{-1} for the composite MnO_2 –CNT films deposited by anodic electrophoretic deposition [30] was much lower compared to the SC of 356 F g^{-1} obtained in this investigation for the films of similar mass.

The results presented in this paper indicated that MnO_2 –CNT nanocomposites have been successfully prepared by CVD and cathodic electrodeposition techniques. The CVD method enabled the CNT growth on the stainless steel meshes. The porous microstructure of CNTs formed on the meshes facilitated the access of MnO_4^- ions to the CNT surface during electrodeposition. Moreover, the porous microstructure of the MnO_2 –CNT nanocomposites was beneficial for the electrolyte access to the active material during testing of the nanocomposites as ES electrodes in the Na_2SO_4 solutions. As a result, the MnO_2 –CNT nanocomposites showed good capacitive behavior, with the highest SC of 356 F g^{-1} at a scan rate of 2 mV s^{-1} . The nanocomposites prepared by CVD and cathodic electrodeposition techniques on low-cost stainless steel mesh

substrates can be considered as possible electrode materials for ESSs.

The authors gratefully acknowledge the financial support of the Natural Sciences and Engineering Research Council of Canada.

- [1] C.-C. Hu, T.-W. Tsou, *Electrochemistry Communications* 4 (2002) 105.
- [2] R.N. Reddy, R.G. Reddy, *Journal of Power Sources* 124 (2003) 330.
- [3] M. Toupin, T. Brousse, D. Belanger, *Chemistry of Materials* 16 (2004) 3184.
- [4] L. Athouel, F. Moser, R. Dugas, O. Crosnier, D. Belanger, T. Brousse, *The Journal of Physical Chemistry C* 112 (2008) 7270.
- [5] V. Khomenko, E. Raymundo-Piñero, F. Béguin, *Journal of Power Sources* 153 (2006) 183.
- [6] R.N. Reddy, R.G. Reddy, *Journal of Power Sources* 132 (2004) 315.
- [7] T. Brousse, M. Toupin, R. Dugas, L. Athouel, O. Crosnier, D. Belanger, *Journal of the Electrochemical Society* 153 (2006) A2171.
- [8] G.-X. Wang, B.-L. Zhang, Z.-L. Yu, M.-Z. Qu, *Solid State Ionics* 176 (2005) 1169.
- [9] E. Beaudrouet, A. Le Gal La Salle, D. Guyomard, *Electrochimica Acta* 54 (2009) 1240.
- [10] M.-S. Wu, P.-C.J. Chiang, *Electrochemical and Solid-State Letters* 7 (2004) A123.
- [11] S.-C. Pang, M.A. Anderson, T.W. Chapman, *Journal of the Electrochemical Society* 147 (2000) 444.
- [12] S.-C. Pang, M.A. Anderson, *Journal of Materials Research* 15 (2000) 2096.
- [13] K.-W. Nam, K.-B. Kim, *Journal of the Electrochemical Society* 153 (2006) A81.
- [14] J.W. Long, A.L. Young, D.R. Rolison, *Journal of the Electrochemical Society* 150 (2003) A1161.
- [15] K. Xia, Q. Gao, J. Jiang, J. Hu, *Carbon* 46 (2008) 1718.
- [16] J. Wei, N. Nagarajan, I. Zhitomirsky, *Journal of Materials Processing Technology* 186 (2007) 356.
- [17] J. Wei, I. Zhitomirsky, *Surface Engineering* 24 (2008) 40.
- [18] F.-J. Liu, *Journal of Power Sources* 182 (2008) 383.
- [19] J. Zhou, J. Cheifitz, R. Li, F. Wang, X. Zhou, T.-K. Sham, X. Sun, Z. Ding, *Carbon* 47 (2009) 829.
- [20] V. Subramanian, H. Zhu, B. Wei, *Electrochemistry Communications* 8 (2006) 827.
- [21] S.I.A. Razak, A.L. Ahmad, S.H.S. Zein, A.R. Boccaccini, *Scripta Materialia* 61 (2009) 592.
- [22] K.-W. Nam, C.-W. Lee, X.-Q. Yang, B.W. Cho, W.-S. Yoon, K.-B. Kim, *Journal of Power Sources* 188 (2009) 323.
- [23] Z. Fan, J. Chen, B. Zhang, B. Liu, X. Zhong, Y. Kuang, *Diamond and Related Materials* 17 (2008) 1943.
- [24] H. Zhang, G. Cao, Z. Wang, Y. Yang, Z. Shi, Z. Gu, *Nano Letters* 8 (2008) 2664.
- [25] G.M. Jacob, I. Zhitomirsky, *Applied Surface Science* 254 (2008) 6671.
- [26] H. Liu, Y. Zhang, D. Arato, R. Li, P. Mérel, X. Sun, *Surface and Coatings Technology* 202 (2008) 4114.
- [27] Y. Zhang, R. Li, H. Liu, X. Sun, P.P. Mérel, S. Déjlets, *Applied Surface Science* 255 (2009) 5003.
- [28] R. Kötz, M. Carlen, *Electrochimica Acta* 45 (2000) 2483.
- [29] B.E. Conway, W.G. Pell, *Journal of Power Sources* 105 (2002) 169.
- [30] J. Li, I. Zhitomirsky, *Journal of Materials Processing Technology* 209 (2009) 3452.
- [31] I. Zhitomirsky, *Advances in Colloid and Interface Science* 97 (2002).